Journal of Micromechanics and Microengineering

Methodology and fabrication of adherent and crack-free SU-8 photoresist-derived carbon MEMS on fused silica transparent substrates

To cite this article before publication: Oscar Pilloni *et al* 2018 *J. Micromech. Microeng.* in press https://doi.org/10.1088/1361-6439/aaf70f

Methodology and Fabrication of Adherent and Crack-free SU-8 Photoresist-derived Carbon MEMS on Fused Silica Transparent Substrates

*Oscar Pilloni [a], Marc Madou [b], Doroteo Mendoza [c], Stephen Muhl [c], Laura Oropeza-Ramos [*d]*

[a] Programa de Maestría y Doctorado en Ingeniería, Universidad Nacional Autónoma de México, CDMX, México.

[b] Department of Mechanical and Aerospace Engineering, University of California, Irvine, USA.

[c] Instituto de Investigaciones en Materiales, Universidad Nacional Autónoma de México, CDMX, México.

[d] Facultad de Ingeniería, Universidad Nacional Autónoma de México, CDMX, México.

[*]Corresponding author:
Laura Oropeza-Ramos
Facultad de Ingeniería, Departamento de Electrónica
Edificio "P" DIE, 3er piso, Anexo de Ingeniería, CU, C.P. 04510 México, CDMX
Tel: (52.55) 5622.31.20, (DIE) 5622.31.12
loropeza@unam.mx

Abstract

Development of carbon based micro electromechanical systems (C-MEMS) has enabled the fabrication of durable, low cost and biocompatible micro devices for specific applications. Thermochemical decomposition of SU-8 (a common photoresist) is often used to fabricate C-MEMS. However, this technique has yielded unreliable results when fabrication on transparent substrates is required due to cracking and detachment of the produced carbon micro structures. We present a methodology for the fabrication of photopatterned carbon films based on SU-8 deposited on transparent fused silica substrates. Specifically, we developed and implemented this methodology for carbon microstructure fabrication derived from SU-8 2035 and SU-8 3035. It was found that SU-8 3035 derived carbon microstructures were crack free and adhered well to the substrate, while SU-8 2035 resulted in fractured and detached carbon microstructures. In addition, we characterized the produced SU-8 3035 derived carbon by measuring its electrical resistivity (1.412 ± 0.011 mΩ m), inter-structure electrical resistance, contact angle ($35.7° \pm 6.0°$), Raman spectrum and adhesion strength to the substrate. In brief, even though SU-8 2035 and SU-8 3035 are useful materials for C-MEMS fabrication, we found that SU-8 3035 is more suitable for the fabrication of crack free and adherent carbon microstructures on transparent fused silica substrates.

Keywords

MEMS; Micro-structure; SU-8; Pyrolysis; Transparent substrate; Carbon.

1. Introduction

Carbon-based micro electromechanical systems (C-MEMS) [1,2] are a collection of technologies that enable the fabrication of carbon microstructures which range from low aspect ratio transparent electrodes [3] to high aspect ratio carbon posts [4] which show desirable properties such as biocompatibility, electrochemical inertness and electrical conduction. C-MEMS are used to build devices for applications in a plethora of fields, such as microfluidics [5], point of care diagnostics [6] and energy storage [7], to list a few.

Although carbon and its allotropes are useful and interesting materials they have proven difficult to pattern in the micro and nano scales. In particular, C-MEMS technology has emerged as a solution by producing devices that use photopatterned pyrolyzed photoresist films (PPF) as building blocks [1,8], with SU-8 photoresist being one of the most popular photo-patternable carbon precursors due to its versatility and ubiquity in traditional MEMS manufacturing.

Moreover, C-MEMS fabrication on transparent substrates enable versatility during the fabrication or the operation of specialized devices when optical transparency is required [9], for example when transmitted light microscopy is desired for observation. Another desirable property for biomedical applications is biocompatibility. Some types of transparent substrates such as fused silica are biocompatible whereas silicon (a common C-MEMS substrate material) has been shown to affect biological and biochemical processes [10–12]. In brief, the useful properties of transparent substrates make them attractive for some application, especially for biomedical and biochemical applications. However, SU-8 derived C-MEMS structure fabrication has been plagued with the vexing problems of cracking and poor adhesion of the PPF to common transparent substrates suitable for pyrolysis [13].

In this paper, we present a methodology for the fabrication of SU-8 derived C-MEMS structures devoid of cracks and well adhered to a transparent substrate. We show that using the more recent SU-8 3035 formulation results in well adhered carbon microstructures whereas the use of the more common SU-8 2035 results in serious adhesion and cracking problems of the PPF. Finally, we report the adhesion strength to the substrate, electrical resistivity, inter-structure electrical resistance, contact angle and Raman spectrum of the produced PPF.

2. Methodology

2.1. Material selection and process outline

Fused silica was selected as substrate material due to its optical transparency, high melting point (which makes it able to withstands the high temperatures needed for the pyrolysis process) and lower cost compared to other alternatives (such as sapphire).

SU-8 2035 and SU-8 3035 photoresists were selected because they are photo-patternable, widely available and suitable for the fabrication of microstructures in sizes ranging from tens to hundreds of micrometers.

We maintained most fabrication parameters constant to show the difference in adhesion due to the photoresists' formulation under the same fabrication and pyrolysis conditions. For this reason, no adhesion promoters where employed and a constant layer thickness was used. A layer thickness of 35 µm was selected because the formulations of both photoresists (SU-8 2035 and 3035) are made specifically to easily achieve this value.

First, samples of SU-8 2035 and SU-8 3035 photoresists were fabricated on the substrate using mask-less photolithography. Secondly, pyrolysis of the photoresists was carried out to obtain the carbon microstructures.

2.2. Photolithography process

2.2.1. Substrate preparation

Fused silica substrates (JGS2 grade, 500 μm thick, UniversityWafer Inc) were cleaned with acetone and isopropyl alcohol and then heated to 230 °C for one hour on a hot plate to dehydrate the surface.

2.2.2. Photoresist coating

Depending on the sample, SU-8 2035 or SU-8 3035 (Microchem) was spin-coated at 3000 rpm on the substrates to obtain 35µm thick layers.

2.2.3. Sample soft bake

The photoresist coated substrates were soft baked on a hotplate using a heating ramp of 10 °C/min from room temperature (18 °C) to the target temperature of 105 °C. The target temperature was maintained constant for 20 minutes. Afterwards, the hot plate was tuned off and the substrates were left to cool down naturally.

2.2.4. Photopatterning

Photoresist patterning was performed in a mask-less photolithography system (SF100 XCEL, Intelligent MicroPatterning) with a resolution of 1.25 µm and a minimum feature size of 5 µm. The system uses a digital micro-mirror device (DMD) to reflect or block the collimated and filtered light of a polychromatic mercury arc lamp. By this means, the digital pattern loaded into

the DMD is transmitted by an optical array to the surface of a target sample [14]. The dose administered is controlled by the time the pattern is exposed to the sample. Exposure time was set to 7.1 s using a wavelength of 365 nm.

2.2.5. Sample post exposure bake

Post exposure bake of the samples was carried on a hotplate using a heating ramp of 10 °C/min from room temperature to the target temperature of 105 °C. The target temperature was held constant for 6 minutes. Then, the hot plate was tuned off and the substrates were left to cool down naturally.

2.2.6. Microstructure development and final bake

Samples were developed for five minutes using SU-8 Developer (Microchem) and a moderate agitation with an orbital shaker. Afterwards, the samples were dried using nitrogen.

The final bake of the samples was performed on a hot plate using a heating ramp of 10°C/min from room temperature to a target temperature of 190 °C. The target temperature was held constant for one hour. Then, temperature was decreased at a rate of 10 °C/min until natural cooling took over and samples were left to reach room temperature. Active cooling was not used during the baking procedures.

2.3. Pyrolysis process

Pyrolysis was performed using a quartz tube furnace (GSL-1100X-UL-LD, MTI) under a constant pure nitrogen (99.99%) flow of 1000 sccm. The target temperature of the process was set to 900 °C, following the temperature profile depicted in Fig. 1 d. The atmosphere was

switched to a forming gas mixture of 95% nitrogen and 5% hydrogen (99.998%) upon reaching the target temperature [15].

After one hour at the target temperature of 900 °C, atmosphere was switched back to pure nitrogen and cooling was performed at a rate equal to or slower than 10 °C/min until the sample reached ambient temperature. Active cooling was not used during this procedure.

Finally, the samples were exposed to a nitrogen stream to clean them of fractured structures that had peeled-off from the substrate.

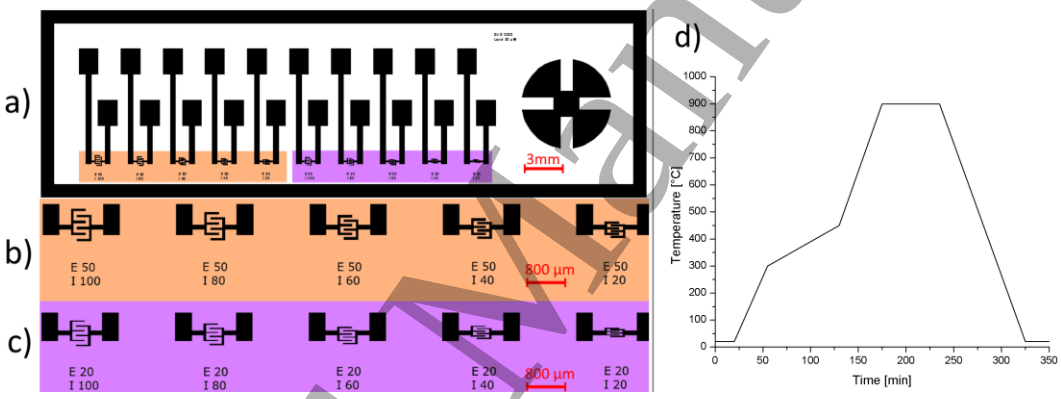

Fig. 1: a) Test pattern used for the pyrolyzed photoresist films (PPF) samples. It consisted of ten arrays of interdigitated electrodes (IDEs) for inter-structure electrical resistance measurement and a cloverleaf shaped structure for electrical resistivity measurement, contact angle and adhesion strength measurements. Detail of the (b)) five IDEs with 50 µm width and interdigit spacing of 100, 80, 60, 40 and 20 µm; and the (c)) five IDEs with 20 µm width and interdigit space of 100, 80, 60, 40 and 20 µm. d) The temperature profile for the pyrolysis process.

3. Results and discussion

The photolithography and pyrolysis processes described above were used to fabricate five carbon samples made of SU-8 2035 and five carbon samples made of SU-8 3035. The test pattern shown in Fig. 1 a-c was used to fabricate the samples. It consisted of ten arrays of interdigitated electrodes (IDEs) for inter-structure electrical resistance measurement (combinations of 50 and 20 μm electrode widths with interdigit spacings of 100, 80, 60, 40 and 20 μm), and a cloverleaf shaped structure for electrical resistivity, contact angle and adhesion strength measurements.

As noted by Martinez-Duarte et. al. [16], the final bake procedure was found to be imperative to maintain adhesion of PPFs to fused silica substrates after pyrolysis. In order to improve the success rate of the pyrolysis, we used a slower ramping rate for the pyrolysis between 300 and 450 °C, which corresponds to the main carbonization of the materials, to accommodate any stress developed in the film during the carbonization [17].

After fabrication, we found that all the SU-8 3035 samples had most of their structures well-adhered to the substrate and with no appreciable fractures observable by optical microscopy or SEM. However, the five SU-8 2035 samples presented mayor cracking and detachment from the substrate, as shown in Fig. 2.

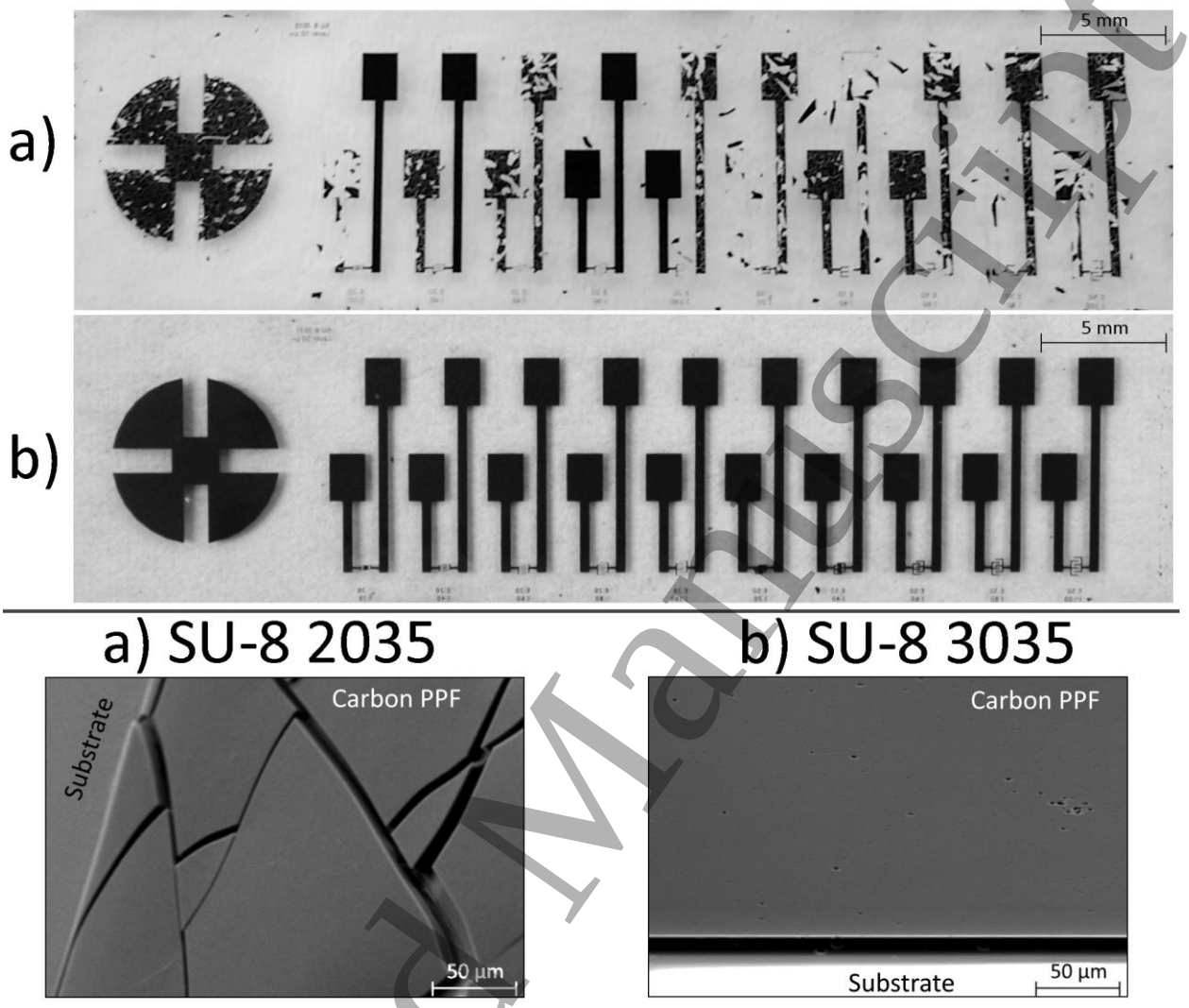

Fig. 2: Optical photograph (top) and SEM (bottom) images of typical samples of pyrolyzed a) SU-8 2035 and b) SU-8 3035. Most, if not all, of the SU-8 2035 structures were fractured and not well-adhered to the substrate after pyrolysis; while SU-8 3035 structures mantained their shape and kept good adhesion to the fused silica substrate.

A possible explanation for the difference in adhesion between SU-8 3035 and 2025 samples stem from the shear analysis performed by the photoresists manufacturer using a similar substrate

material (quartz). This analysis showed that SU-8 3035 and SU-8 2035 films had adhesion strengths of 80 MPa and 61 MPa, respectively [18].

The SU-8 2035 weaker adhesion strength prior to pyrolysis, in addition to the thermal stresses introduced during the pyrolysis process, could be the cause of the observed detachment and cracking of the PPF. This might mean that the bonding strength of the carbon structure to the substrate could be dependent on the adhesion of the carbon precursor to the substrate before pyrolysis. To explore this, measurements of adhesion to the substrate were conducted for both photoresists before and after pyrolysis.

Given that all SU-8 2035 samples presented mayor detachment and cracking problems, measurements of electrical resistivity, inter-structure electrical resistance, contact angle and Raman spectrum were only performed on the SU-8 3035 samples. Measurements of adhesion strength to the substrate were carried in the SU-8 2035 structures that remained adhered and intact after pyrolysis.

3.1. Adhesion strength to the substrate

SU-8 3035 and SU-8 2035 PPF adhesion to the fused silica substrate was tested using micro-scratch testing and sonication before and after pyrolysis.

The scratch test consists of a moving load applied by a counter body of known shape and size to a film or coating. To assess the adhesion force, the load is increased until a critical value where the film detaches from the substrate. This critical load is a function of film-substrate adhesion, flaw size distribution at substrate-film interface, mechanical properties of substrate and film, film thickness, counter body tip radius, loading rate, internal stress in coating, and friction between counter body tip and coating [19–23].

First, samples were subjected to a variable-load scratch test (0.2 to 15 N at a loading rate of 7.5 N/min) using a micro-scratch tribometer (Nanovea, PB1000) and a 200 µm diameter spherical diamond tip as the counter body. Measurements of the SU-8 2035 PPF were carried on the few adherent structures that withstood the pyrolysis process. Fig. 3 summarizes these data points obtained. Also, scratch tests were made for both photoresists deposited in a silicon substrate as control experiments for comparison.

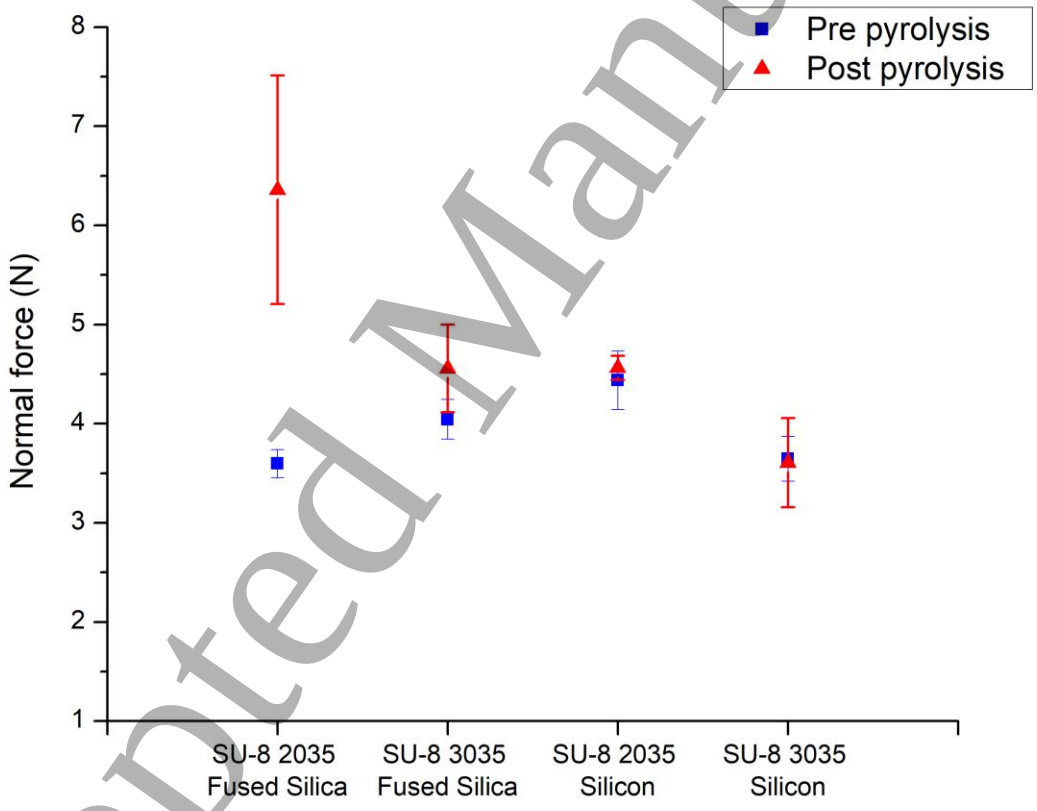

Fig. 3: Critical load (normal force) required to delaminate the photoresists films from their substrate. Measurements for before and after pyrolysis process are provided.

Secondly, samples were submerged in deionized water and treated in an ultrasonic bath for five minutes. Optical microscopy was used to search for cracked or detached structures. However, no appreciable changes were found in any SU-8 3035 sample, before or after pyrolysis. That is, structures remained intact and well-adhered to the fused silica substrate. This constitutes a significant improvement over similar tests made in previous works [13]. On the other hand, SU-8 2035 structures showed complete to partial detachment, with only a few structures remaining adherent to the substrate. This behavior occurred to SU-8 2035 structures both before and after pyrolysis. Photographs of this test are provided in a supplementary information document.

These results indicate that the produced PPF adhesion to the substrate after pyrolysis may be independent from its adhesion to fused silica but closely related for silicon before the process, and that this parameter may not be related to the cracking problems of the PPF due to it being similar for both photoresists. However, the severe delamination problems presented by SU-8 2035 during sonication suggests that the interface of the photoresist to substrate is highly susceptible to humidity and vibration, whereas SU-8 3035 remained impervious to the test. This property of SU-8 3035 PPFs may prove useful for cleaning procedures, or for the intended operation of devices fabricated with the proposed method.

3.2. Electrical resistivity

Van der Pauw [24] resistivity measurements of the pyrolyzed films were carried out using a source meter (Keithley 2636B) connected to the cloverleaf shaped structure shown in Fig. 1. An average resistivity of 1.412 ± 0.011 mΩ m was measured across all pyrolyzed SU-8 3035 samples.

The measured resistivity is comparable to previous electrical measurements of original SU-8 formulation, and polyimide-derived carbon PPFs [13,25]. This makes the obtained material useful for devices that require electrical conductivity, such as microelectrode arrays.

3.3. Inter-structure electrical resistance

As pointed out by Matias et. al. [26], sometimes the C-MEMS process results in undesirable residual conducting carbon layers in areas originally designed to be insulating. Interdigitated electrodes with varying inter-electrode spacing (Fig. 4) were used to measure the inter-structure electrical resistance resulting from such spurious layers produced by the proposed methodology.

Spacing equal or greater than 40 μm between electrodes resulted in electrically isolated structures, with electrical resistances higher than what we were able to measure ($> 10^9$ Ω, Fluke 116). Electrodes with 20 μm inter-structure spacing resulted in electrically connected structures, showing electrical resistances of 10^3 Ω.

This likely indicates that the combination of the careful selection of inter-microstructure spacing, and the good adhesion of the carbon film to the substrate could influence the reproducibility of devices free of residual layer without the need for further processing.

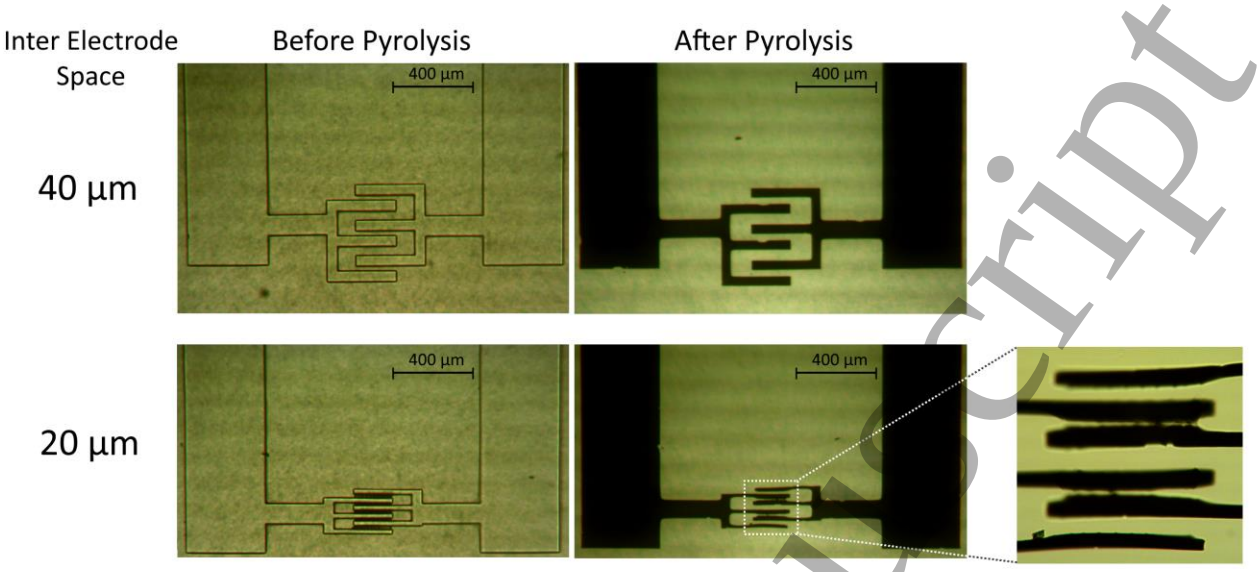

Fig. 4: SU-8 3035 interdigitated electrodes (IDEs) before and after pyrolysis. IDEs with an inter-structure spacing equal or greater than 40 µm were electrically isolated from adjacent features, whereas features with 20 µm separations were electrically connected (bonded by residual material trapped in between the IDEs).

3.4. Raman spectroscopy

Raman spectroscopy has been proven to reliably obtain microstructural information of thin carbon films[27]. For this reason, Raman spectra of the SU-8 3035 samples were obtained. We measured the spectra at 3 different locations on each sample, using a 532 nm wavelength laser Raman microscope (DXR, Thermo Scientific). The wavenumber for the G band (associated with the graphitic content of the PPF) was found at 1591.7 ±2.55 cm^{-1} and the D band (associated with the level of disorder of the carbon lattice) was found at 1333.5 ±2.25 cm^{-1} (Fig. 5 a-b). We calculated an average D to G band intensity ratio (ID/IG) of 0.9694 ±0.0503.

These results suggest that the achieved material is comparable to glassy carbon, which is a useful type of carbon for electrochemical applications [2,7]. All samples showed homogenous Raman spectra across each sample (Fig. 5 a) and overall (Fig. 5 b), which shows that the proposed methodology can produce a uniform and highly reproducible material.

3.5. Contact angle measurements

A set of contact angle measurements were made to investigate the carbon hydrophobicity. We used 38 µl droplets of deionized water on the carbon surface of the SU-8 3035 samples and measured an average contact angle of 35.7° ± 6.0°. A representative measurement is shown in Fig. 5 c.

Previous reports have shown that the contact angle of SU-8 derived PPFs is affected by post-carbonization surface treatments and various fabrication variables, such as the pyrolysis atmosphere [28]. Furthermore, measurements performed by C. S. Sharma on pyrolyzed SU-8 2000 films showed post pyrolysis angles of around 70°[29]. The variables that could have affected this angle include the photoresist formulation, and therefore the pyrolysis by-products, and the inert atmosphere used during pyrolysis.

Although both Sharma's and our results indicate a hydrophilic surface, our samples had a contact angle that was roughly half of that reported immediately after fabrication. This makes the obtained microstructured carbon attractive for applications that require a hydrophilic surface without the need of further surface treatment.

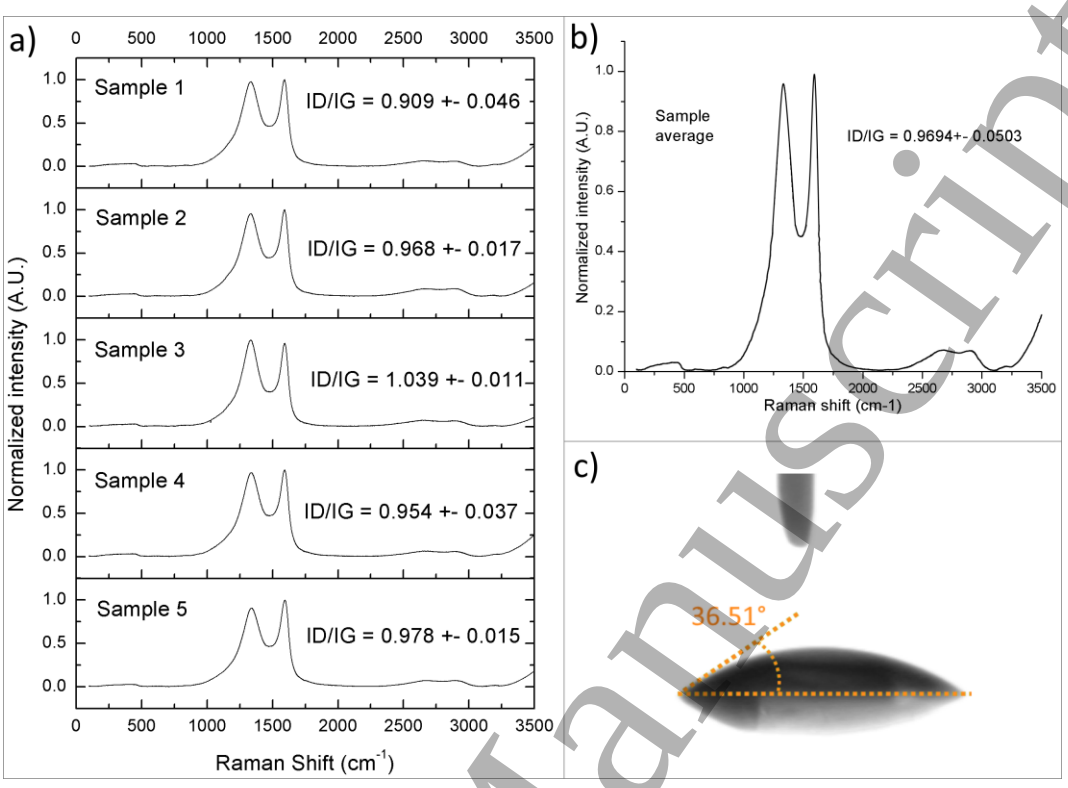

Fig. 5: Average Raman spectra obtained from pyrolyzed SU-8 3035 for a) each sample (n=3) and b) overall (n=15). Intensity ratios of D and G peaks (ID/IG) are shown for each sample and an overall average. c) A contact angle measurement made on the PPF. The dark blob is water, the tip at the top is the liquid dispenser and the gray area below the dotted line results from the droplet's reflection on the carbon surface.

4. Conclusions

We have shown that the proposed methodology is suitable for the fabrication of SU-8 3035 derived C-MEMS microstructures devoid of cracks which have good adhesion to transparent substrates.

In brief, SU-8 3035 was found more suitable to produce adherent carbon microstructures on transparent fused silica substrates, while SU-8 2035 yields fractured and detached

microstructures following the same fabrication methodology. Both photoresists presented similar adhesion strength to fused silica before and after pyrolysis, but SU-8 2035 interface to the substrate showed mayor susceptibility to water resulting in the detachment of the film from the substrate. This suggests that the exposure of SU-8 2035 films to ambient humidity may play a determining factor for the success or failure of the fabrication of C-MEMS devices based on that photoresist built on fused silica.

In conclusion, the low resistivity, hydrophilic contact angle, lack of cracking, good adhesion and lack of susceptibility to water of the interface to fused silica of SU-8 3035 derived PPF produced with the proposed method provides enough design flexibility to build novel C-MEMS on transparent substrates for applications that require optical transparency, such as biomedical, medical or biological applications requiring the use of optical microscopy with transmitted illumination for the inspection of samples.

Author Contributions

The manuscript was written with contributions from all the authors. All authors have given approval to the final version of the manuscript.

Acknowledgements

This work was funded by DGAPA-PAPIIT-UNAM [grant number IN115116] and by CONACYT-UNAM [project number 269280] for the acquisition of the Nanovea tribometer. Partially funded by CONACYT Fronteras de la Cienca [grant number 344] and PAPIIT [grant number IN106316]. The first author was supported by CONACYT scholarship [scholarship number 487698], and we also would like to thank Ing. Ma. Cristina Zorrilla Cangas from the

Laboratorio de Materiales Avanzados, Instituto de Física, UNAM for her assistance in the Raman spectroscopy.

Competing Interests

The authors declare that they have no competing interests.

References

[1] Wang C and Madou M 2005 From MEMS to NEMS with carbon *Biosens. Bioelectron.* **20** 2181–7.

[2] Ranganathan S, McCreery R, Majji S M and Madou M 2000 Photoresist-Derived Carbon for Microelectromechanical Systems and Electrochemical Applications *J. Electrochem. Soc.* **147** 277.

[3] Donner S, Li H W, Yeung E S and Porter M D 2006 Fabrication of optically transparent carbon electrodes by the pyrolysis of photoresist films: Approach to single-molecule spectroelectrochemistry *Anal. Chem.* **78** 2816–22.

[4] Wang C, Jia G, Taherabadi L H and Madou M J 2005 A novel method for the fabrication of high-aspect ratio C-MEMS structures *J. Microelectromechanical Syst.* **14** 348–58.

[5] Rouabah H a, Park B Y, Zaouk R B, Morgan H, Madou M J and Green N G 2011 Design and fabrication of an ac-electro-osmosis micropump with 3D high-aspect-ratio electrodes using only SU-8 *J. Micromechanics Microengineering* **21** 035018.

[6] Martinez-Duarte R, Gorkin R a, Abi-Samra K and Madou M J 2010 The integration of 3D carbon-electrode dielectrophoresis on a CD-like centrifugal microfluidic platform. *Lab Chip* **10** 1030–43.

[7] Wang C, Taherabadi L, Jia G, Madou M, Yeh Y and Dunn B 2004 C-MEMS for the Manufacture of 3D Microbatteries *Electrochem. Solid-State Lett.* **7** A435.

[8] Pilloni O, Benítez Benítez J L and Oropeza-Ramos L 2016 Micro Device for Bio-Particle Positioning in a 3D space based on Carbon MEMS and Dielectrophoretic Forces *ECS Trans.* **72** 17–24.

[9] Martinez-Duarte R 2014 SU-8 Photolithography as a Toolbox for Carbon MEMS *Micromachines* **5** 766–82.

[10] Steinhauer C, Ressine A, Marko-Varga G, Laurell T, Borrebaeck C A K and Wingren C 2005 Biocompatibility of surfaces for antibody microarrays: Design of macroporous silicon substrates *Anal. Biochem.* **341** 204–13.

[11] Coletti C, Jaroszeski M J, Pallaoro A, Hoff A M, Iannotta S and Saddow S E 2007 Biocompatibility and wettability of crystalline SiC and Si surfaces *Annu. Int. Conf. IEEE Eng. Med. Biol. - Proc.* 5849–52.

[12] Ni M, Tong W H, Choudhury D, Rahim N A A, Iliescu C and Yu H 2009 Cell culture on MEMS platforms: A review. *Int. J. Mol. Sci.* **10** 5411–41.

[13] Singh A, Jayaram J, Madou M and Akbar S 2002 Pyrolysis of Negative Photoresists to Fabricate Carbon Structures for Microelectromechanical Systems and Electrochemical Applications *J. Electrochem. Soc.* **149** E78.

[14] Xiang N, Yi H, Chen K, Wang S and Ni Z 2013 Investigation of the maskless lithography technique for the rapid and cost-effective prototyping of microfluidic devices in laboratories *J. Micromechanics Microengineering* **23.**

[15] Pilloni O, Benítez J L B, Olguín L F, Palacios-Morales C A and Oropeza-Ramos L 2016 Micro Device for Bio-Particle Positioning in a 3D space based on Carbon MEMS and Dielectrophoretic Forces *ECS Transactions* vol 72.

[16] Martinez-Duarte R, Renaud P and Madou M J 2011 A novel approach to dielectrophoresis using carbon electrodes *Electrophoresis* **32** 2385–92.

[17] G. M. Jenkins K K 1976 *Polymeric Carbons: Carbon Fibre, Glass and Char* (Cambridge University Press).

[18] Microchem SU-8 Table of properties.

[19] Bull S J 1997 Failure Mode Maps in the Thin Scratch Adhesion Test *Tribol. Int.* **30.**

[20] Kutilek P and Miksovsky J 2011 The procedure of evaluating the practical adhesion strength of new biocompatible nano-and micro-thin films in accordance with international standards *Acta Bioeng. Biomech.* **13** 87–94.

[21] Bull S J 1991 Failure Modes in Scratch Adhesion Testing *Surf. Coatings Technol.* **50** 25–32.

[22] Mittal K L 1976 Adhesion Measurement of Thin Films *Electrocompon. Sci. Technol.* **3** 21–42.

[23] Matthewson M J 1986 Adhesion measurement of thin films by indentation *Appl. Phys. Lett.* **49** 1426.

[24] van der Pauw L J 1958 A method of measuring the resistivity and hall coefficient of discs of arbitrary shape *Philips Res. Reports* **13** 1–9.

[25] Park B Y, Taherabadi L, Wang C, Zoval J and Madou M J 2005 Electrical Properties and

Shrinkage of Carbonized Photoresist Films and the Implications for Carbon Microelectromechanical Systems Devices in Conductive Media *J. Electrochem. Soc.* **152** J136.

[26] Vázquez Piñón M, Cárdenas Benítez B, Pramanick B, Perez-Gonzalez V H, Madou M J, Martinez-Chapa S O and Hwang H 2017 Direct current-induced breakdown to enhance reproducibility and performance of carbon-based interdigitated electrode arrays for AC electroosmotic micropumps *Sensors Actuators, A Phys.* **262** 10–7.

[27] Tuinstra F and Koenig J L 1970 Raman Spectrum of Graphite *J. Chem. Phys.* **53** 1126–30.

[28] Hsia B, Kim M S, Vincent M, Carraro C and Maboudian R 2013 Photoresist-derived porous carbon for on-chip micro-supercapacitors *Carbon N. Y.* **57** 395–400.

[29] Sharma C S, Sharma A and Madou M 2010 Multiscale carbon structures fabricated by direct micropatterning of electrospun mats of SU-8 photoresist nanofibers *Langmuir* **26** 2218–22.